

Sign-Reversing Orbital Polarization in the Nematic Phase of FeSe Driven by Aslamazov-Larkin Processes

Seiichiro ONARI¹, Youichi YAMAKAWA², and Hiroshi KONTANI²

¹ *Department of Physics, Okayama University, Okayama 700-8530, Japan.*

² *Department of Physics, Nagoya University, Furo-cho, Nagoya 464-8602, Japan.*

(Dated: January 27, 2023)

Nontrivial \mathbf{k} -dependence of the orbital polarization ($\Delta E_{xz}(\mathbf{k})$, $\Delta E_{yz}(\mathbf{k})$) in the orthorhombic phase, such as the sign-reversal of the orbital splitting between Γ - and X-points in FeSe, provides significant information to understand the nematicity in Fe-based superconductors. To solve this problem, we analyze the multiorbital Hubbard models in the orbital-ordered state by extending the orbital-spin fluctuation theory. The present theory describes the spontaneous symmetry breaking with respect to the orbital polarization and spin susceptibility self-consistently. In the orbital-ordered state in FeSe, we obtain the two Dirac cone Fermi pockets in addition to the sign-reversing orbital polarization, consistently with experiments. The orbital-order in Fe-based superconductors originates from the strong orbital-spin interplay due to the Aslamazov-Larkin processes.

PACS numbers: 74.70.Xa, 75.25.Dk, 74.20.Pq

The spontaneous symmetry breaking from C_4 - to C_2 -symmetry, so called the electronic nematic transition, is one of the fundamental unsolved electronic properties in Fe-based superconductors. To explain this nematicity, both the spin-nematic scenario [1–4] and the orbital order scenario [5–11] have been studied intensively. Above the structural transition temperatures T_{str} , large enhancement of the electronic nematic susceptibility predicted by both scenarios [1, 8] is actually observed by the measurements of the softening of the shear modulus C_{66} [1, 8, 12, 13], Raman spectroscopy, [14–16], and in-plane resistivity anisotropy $\Delta\rho$ [17].

To investigate the origin of the nematicity, FeSe ($T_c = 9$ K) is a favorable system since the electronic nematic state without magnetization is realized below $T_{\text{str}} = 90$ K down to 0 K. Above T_{str} , the strength of the antiferromagnetic fluctuations is very weak according to the NMR [18, 19] and neutron scattering [20, 21] studies, in contrast to the strong spin fluctuations above T_{str} in LaFeAsO [22] and BaFe₂As₂ [23]. This fact means that the magnetism is not a necessary condition for the electronic nematic state. In contrast to the smallness of the spin fluctuations, large nematic susceptibility is measured by C_{66} and $\Delta\rho$ in FeSe. Based on the orbital-spin fluctuation theory, called the self-consistent vertex-correction (SC-VC) theory, the development of the strong orbital fluctuations in FeSe are explained even when the spin-fluctuations are very small, consistently with experimental reports in FeSe [24]. The origin of the strong orbital fluctuations in FeSe is the Aslamazov-Larkin vertex correction (AL-VC) that describes the orbital-spin mode-coupling [8].

The nontrivial electronic state below T_{str} gives a crucial test for the theories proposed so far. In the orthogonal phase with $(a - b)/(a + b) \sim 0.3\%$, large orbital-splitting $|E_{xz} - E_{yz}|$ of order 50 meV is observed at X-point by ARPES studies in BaFe₂As₂ [25], NaFeAs [26],

and FeSe [27–35]. Especially, noticeable deformation of the Fermi surfaces (FSs) with C_2 -symmetry is realized in FeSe, because of the smallness of the Fermi momenta. In FeSe, the orbital splitting $E_{xz} - E_{yz}$ at Γ -point is positive, oppositely to the negative splitting at X-point, as reported in Ref. [33]. This sign-reversing orbital splitting is not realized in the non-magnetic orthorhombic phase in NaFeAs [26]. In addition, the e-FS1 at X-point is deformed to two Dirac cone Fermi pockets in thin-film FeSe [32, 35]. The aim of this study is to explain these non-trivial electronic states in the orbital-ordered states by extending the SC-VC theory in the orbital-ordered state.

Microscopically, the orbital order is expressed by the symmetry breaking in the self-energy. In the mean-field level approximations, however, the self-energy is constant in \mathbf{k} -space unless large inter-site Coulomb interactions are introduced as studied in Ref. [11]. Therefore, we study the non-local correlation effect on the self-energy beyond the mean-field theory based on the realistic Hubbard model with on-site Coulomb interaction. The strong positive feedback between the nematic orbital order and C_2 -symmetric spin susceptibility plays essential roles.

In this paper, we study the origin of the orbital order in Fe-based superconductors, by considering the spontaneous symmetry breaking in both self-energy and spin susceptibility self-consistently. Experimentally observed strong \mathbf{k} -dependent orbital polarization ($\Delta E_{xz}(\mathbf{k})$, $\Delta E_{yz}(\mathbf{k})$) is given by the non-local self-energy with C_2 -symmetry. In the FeSe model, we obtain the sign-reversing orbital-splitting $E_{xz} - E_{yz}$ between Γ - and X-points reported in Refs. [33], in addition to the two Dirac-cone Fermi pockets around X-point when U is larger [32, 35]. Thus, important experimental electronic properties in the orbital-ordered phase are well understood thanks to the AL-VC.

Here, we study the realistic eight-orbital d - p Hubbard models $H_M(r) = H_M^0 + rH_M^U$ ($M = \text{LaFeAsO}$ and FeSe)

introduced in our previous study [24]. Figures 1 show the bandstructures and the Fermi surfaces (FSs) in the FeSe and LaFeAsO models. In FeSe, the BCS-BEC crossover is suggested experimentally since each Fermi pocket is very shallow [36]. As for the Coulomb interaction H_M^U , we use the first-principles screened Coulomb potential given in Ref. [37]: The averaged Coulomb interaction is $\bar{U} = 7.21$ eV for FeSe, which is much larger than $\bar{U} = 4.23$ eV for LaFeAsO because of the small screening effect on U in FeSe [37]. For this reason, the ratio between the Hund's and Coulomb interactions in FeSe, $\bar{J}/\bar{U} = 0.0945$, is much smaller than the ratio $\bar{J}/\bar{U} = 0.134$ in LaFeAsO. Hereafter, the five d -orbitals $d_{3z^2-r^2}$, d_{xz} , d_{yz} , d_{xy} , $d_{x^2-y^2}$ are denoted as 1, 2, 3, 4, 5.

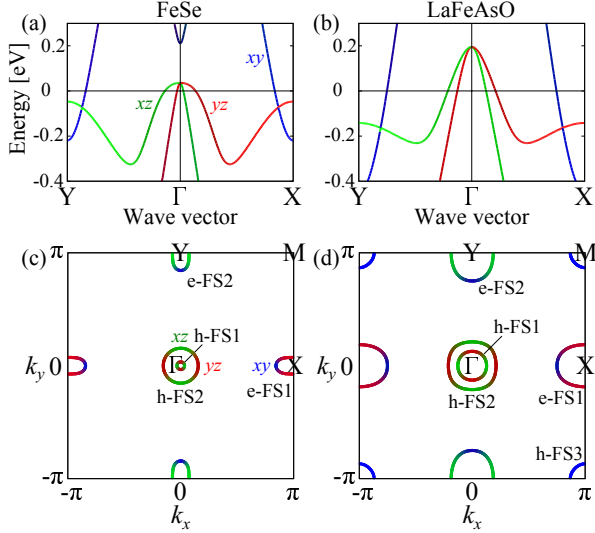


FIG. 1: Bandstructures of the eight-orbital tight-binding models for the (a) FeSe and (b) LaFeAsO models in the unfolded Brillouin zone. FSs for the FeSe and LaFeAsO models are shown in (c) and (d), respectively. The colors correspond to 2 (green), 3 (red), and 4 (blue), respectively.

In the present study, we calculate the \mathbf{k} -dependence of the self-energy on the basis of the self-consistent one-loop approximation. The Green function in the orbital basis is given as

$$\hat{G}(\mathbf{k}) = (\hat{z}^{-1}i\epsilon_n + \mu - \hat{h}_M^0(\mathbf{k}) - \Delta\hat{\Sigma}(\mathbf{k}))^{-1}, \quad (1)$$

where $\hat{h}_M^0(\mathbf{k})$ is the kinetic term, $\Delta\hat{\Sigma}(\mathbf{k})$ is symmetry breaking self-energy, and \hat{z}^{-1} is the diagonal mass-enhancement factor. We put $1/z_l = 1$ for $l \neq 4$, and $1/z_4 = 3$ (2) for FeSe (LaFeAsO) to represent the strong renormalization of the d_{xy} -orbital band [27]. The self-energy in the one-loop approximation is given as

$$\begin{aligned} \Sigma_{l,\nu}(k) = & - \sum_{m,m'} \Gamma_{l,\nu;m',m}^c \Delta n_{m,m'} \\ & + T \sum_{q,m,m'} V_{l,m;\nu',m'}^\Sigma(q) G_{m,m'}(k-q), \quad (2) \end{aligned}$$

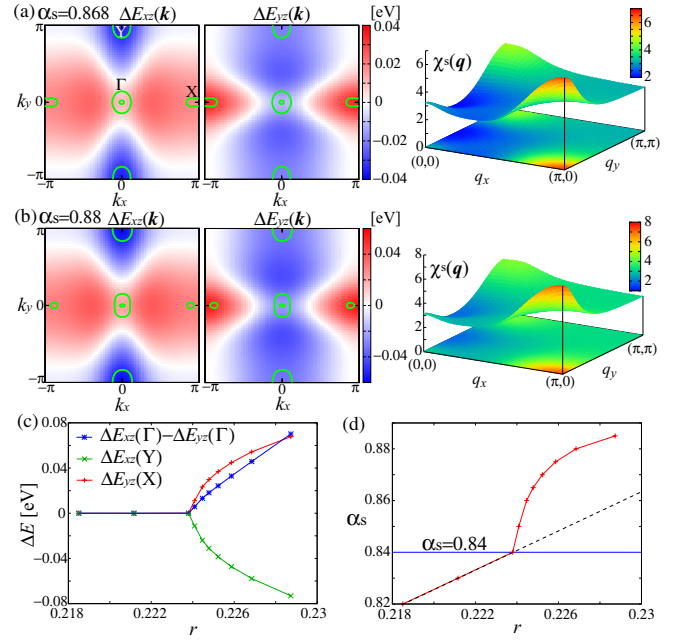


FIG. 2: (color online) Nematic orbital polarization ($\Delta E_{xz}(\mathbf{k})$, $\Delta E_{yz}(\mathbf{k})$) and the spin susceptibility in the FeSe model for (a) $\alpha_s = 0.868$ ($r = 0.225$) and (b) $\alpha_s = 0.88$ ($r = 0.227$). The realized FSs are shown by the green lines. The orbital splitting $E_{xz} - E_{yz}$ at Γ -point is positive, as observed experimentally. We also show the r -dependences of (c) $\Delta E_{xz}(\Gamma) - \Delta E_{yz}(\Gamma)$, $\Delta E_{xz}(Y)$, and $\Delta E_{yz}(X)$, and (d) α_s for $0.229 > r > 0.219$ ($0.885 \geq \alpha_s \geq 0.82$).

where $\Delta n_{m,m'} \equiv \langle c_{i,m,\sigma}^\dagger c_{i,m',\sigma} \rangle - \langle c_{i,m,\sigma}^\dagger c_{i,m',\sigma} \rangle_0$, and $\hat{\Gamma}^c$ is the bare Coulomb interaction for the charge-channel in Ref. [8, 9]. The non-local interaction $\hat{V}^\Sigma(q)$ is given as

$$\hat{V}^\Sigma(q) = \frac{3}{2} \hat{\Gamma}^s \hat{\chi}^s(q) \hat{\Gamma}^s + \frac{1}{2} \hat{\Gamma}^c \hat{\chi}^c(q) \hat{\Gamma}^c, \quad (3)$$

where $\hat{\chi}^{s,c}(q) = \hat{\chi}^0(q)(1 - \hat{\Gamma}^{s,c} \hat{\chi}^0(q))^{-1}$ and $\chi_{l,\nu',m,m'}^0(q) = -T \sum_k G_{l,m}(k+q) G_{m',\nu'}(k)$. Note that the over-counting term in the second-order self-energy correction should be subtracted.

From Eq. (2), the B_{1g} -type symmetry breaking self-energy included in Eq. (1), which is orbital-diagonal, is derived as

$$\Delta \Sigma_l(\mathbf{k}) = \text{Re} \left\{ \Sigma_{l,l}(\mathbf{k}, \epsilon_n) - \Sigma_l^{A_{1g}}(\mathbf{k}, \epsilon_n) \right\}_{i\epsilon_n \rightarrow 0} \quad (4)$$

for $l = 2, 3$, where $\Sigma_l^{A_{1g}}(k) \equiv (\Sigma_{l,l}(k) + \Sigma_{5-l,5-l}(k'))/2$ ($\mathbf{k}' = (k_y, k_x)$) is the A_{1g} -component of the self-energy. In the present study, we calculate Eqs. (2)-(4) self-consistently. We find that the symmetry breaking self-energy emerges with increasing the prefactor of the Coulomb interaction r [38].

First, we explain the numerical results for the FeSe model, using 64×64 \mathbf{k} -meshes and 512 Matsubara frequencies at $T = 50$ meV. In FeSe, the orbital order with $\Delta E_{xz}(\mathbf{k}) \equiv \Delta \Sigma_2(\mathbf{k})$ and $\Delta E_{yz}(\mathbf{k}) \equiv \Delta \Sigma_3(\mathbf{k})$

emerges when the spin Stoner factor α_S , which is the maximum eigenvalue of $\Gamma^s \chi^0(\mathbf{q})$, is larger than 0.84 ($r > 0.224$). The magnetic order is realized when $\alpha_S = 1$. In Fig. 2, we show the obtained orbital polarization ($\Delta E_{xz}(\mathbf{k})$, $\Delta E_{yz}(\mathbf{k})$) and the spin susceptibility $\chi^s(\mathbf{q}) \equiv \sum_{l,m} \chi_{l,l;m,m}^s(\mathbf{q})$ for (a) $\alpha_S = 0.868$ and (b) $\alpha_S = 0.88$. Due to the positive $\Delta E_{yz}(X)$, the size of the e-FS1 around X-point is reduced, and two Dirac-cone Fermi pockets appear in Fig. 2 (b). Another electron-pocket around Y-point, e-FS2, is enlarged by the negative $\Delta E_{xz}(Y)$. In addition, the hole-pockets are also deformed to be ellipsoidal due to positive $\Delta E_{xz}(\Gamma) - \Delta E_{yz}(\Gamma)$: The h-FS2 is elongated along the k_y -axis, consistently with the observation in Ref. [33]. Due to the orbital polarization, the in-plane spin susceptibility anisotropy $\chi^s(\pi, 0) > \chi^s(0, \pi)$ is obtained self-consistently, as shown in Fig. 2 (a) and (b) [39].

In Fig. 2 (c), we show the r -dependences of the orbital-order parameters $\Delta E_{xz}(\Gamma) - \Delta E_{yz}(\Gamma)$, $\Delta E_{xz}(Y)$, and $\Delta E_{yz}(X)$. We see that the orbital order appears as a second-order transition at $\alpha_S = 0.84$, the relations $\Delta E_{xz}(Y) < 0$ and $\Delta E_{yz}(X) > 0$ are realized in the ordered state. Interestingly, the orbital splitting at Γ -point, $E_{xz} - E_{yz}$, is positive, and therefore h-FS2 is elongated along the k_y -axis. The electron-numbers of d_{xz} - and d_{yz} -orbitals at $\alpha_S = 0.88$ are $n_{xz} = 1.32$ and $n_{yz} = 1.31$, respectively: The difference $n_{xz} - n_{yz} \sim +10^{-2}$ will induce the small lattice deformation $(a-b)/(a+b) \approx 0.2\%$ in FeSe due to small e -ph interaction.

We also show the r -dependence of α_S in Fig. 2 (d). Although α_S increases linearly with r , in the absence of the orbital order ($\alpha_S < 0.84$), the spin fluctuations are drastically enlarged when the orbital order appears ($\alpha_S > 0.84$) as predicted in Ref. [39]. However, the increment of α_S is suppressed for $\alpha_S \gtrsim 0.87$ because of the bad intra- d_{yz} -orbital nesting at $\mathbf{q} \sim (\pi, 0)$ due to positive $E_{xz} - E_{yz}$ at Γ -point [33]. Such sign-reversal does not occur in the LaFeAsO model.

In Figs. 3, we display the obtained bandstructures and orbital polarization in the FeSe model for (a) $\alpha_S = 0.868$ and (b) $\alpha_S = 0.88$. In both cases, the orbital splitting $E_{xz}(Y) - E_{yz}(X)$ is negative, whereas $E_{xz}(\Gamma) - E_{yz}(\Gamma)$ is positive. The corresponding FSs are also shown in Figs. 3 (c) and (d), respectively. The present results indicates that the shape of the hole-pocket in Fig. 3 (c) might be realized at the temperatures just below T_{str} .

Here, we explain why the sign-reversing orbital polarization appears in FeSe based on the approximate expression $\Delta E_l(\mathbf{k}) = \Delta \Sigma_l(\mathbf{k}) \sim T \sum_{\mathbf{q}} (\mu - E_{l,\mathbf{k}+\mathbf{q}})^{-1} V_l^\Sigma(\mathbf{q}, 0)$, where $E_{l,\mathbf{k}}$ is the l -orbital character band energy. Since $V_3^\Sigma(\mathbf{q}, 0)$ is large at $\mathbf{q} \sim (\pi, 0)$, $\Delta E_{yz}(\Gamma) < 0$ is realized due to the large d_{yz} -orbital weight on the electron-band around the X-point above the Fermi level; see Fig. 1 (c). As a result, $E_{xz}(\Gamma) - E_{yz}(\Gamma)$ is positive in FeSe, in which both hole- and electron-pockets are very shallow. As shown later, $\Delta E_l(\mathbf{k})$ in the LaFeAsO model with large

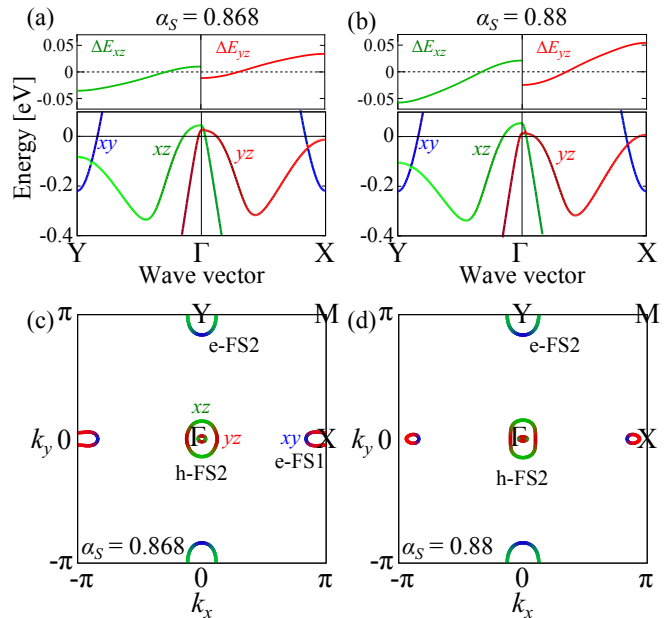


FIG. 3: (color online) Orbital polarizations and bandstructures in the FeSe model along $Y \rightarrow \Gamma \rightarrow X$ for (a) $\alpha_S = 0.868$ and (b) $\alpha_S = 0.88$. The corresponding FSs are shown in (c) and (d), respectively.

FSs is very different from that in the FeSe model.

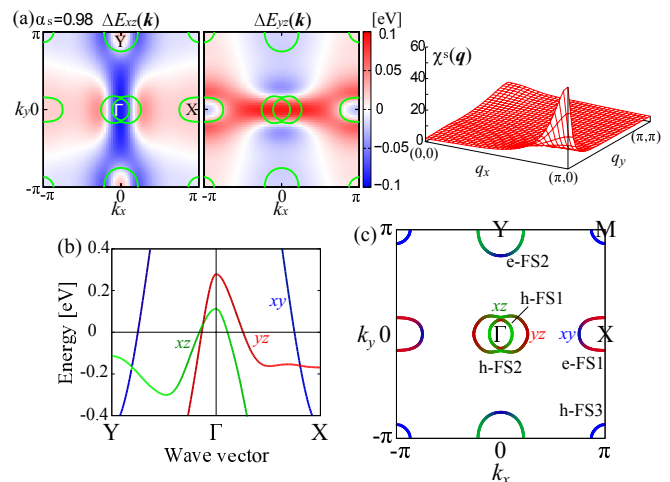


FIG. 4: (color online) (a) Obtained orbital polarization ($\Delta E_{xz}(\mathbf{k})$, $\Delta E_{yz}(\mathbf{k})$) and the spin susceptibility in the LaFeAsO model for $\alpha_S = 0.98$ ($r = 0.390$). The realized FSs are shown by the green lines. The bandstructures and the orbital character of the FSs at $\alpha_S = 0.98$ are shown in (b) and (c), respectively.

Next, we show the numerical results for the LaFeAsO model with $z_4^{-1} = 2$. Then, the orbital order is realized for $\alpha_S \gtrsim 0.93$. In Fig. 4 (a), we show the obtained orbital polarization at $\alpha_S = 0.98$. The e-FS1 around X-point is smaller than e-FS2 around Y-point due to the orbital polarization $\Delta E_{xz}(Y) < 0$ and $\Delta E_{yz}(X) > 0$.

At the same time, the outer hole-pocket (h-FS2) is elongated along the k_x -axis, due to the negative orbital splitting $E_{xz} - E_{yz}$ at Γ -point. This result is consistent with the Fermi surface deformation in the non-magnetic orthorhombic phase in NaFeAs [26]. For the better agreement, realistic NaFeAs model with the spin-orbit interaction should be analyzed. In the ordered state, strong in-plane anisotropy of the spin susceptibility with $\chi^s(\pi, 0) \gg \chi^s(0, \pi)$ is induced [39], consistently with the neutron inelastic scattering experiments. The obtained bandstructures and the orbital character of the FSs are shown in Fig 4 (b) and (c), respectively.

In both FeSe and LaFeAsO models, the obtained orbital polarization ($E_{xz}(\mathbf{k}), E_{yz}(\mathbf{k})$) has some similarity to the d -wave form factor [11, 31]. In addition, the significant orbital polarization appears around the Γ -point in the present study. Note that e-FSs is deformed by the potentials $\Delta E_{xz}(Y)$ and $\Delta E_{yz}(X)$, whereas $\Delta E_{xz}(X)$ and $\Delta E_{yz}(Y)$ are not important for the FS deformation.

In Ref. [24], the present authors studied the present models using the SC-VC theory, and found that the orbital order is realized when $\alpha_S = 0.86$ ($\alpha_S = 0.95$) in the FeSe model with $z_4^{-1} = 3$ (LaFeAsO model with $z_4^{-1} = 2$). These spin Stoner factors are almost equal to those obtained in the present theory. In FeSe, the orbital order is realized even when the spin fluctuations are weak in FeSe ($\alpha_S \gtrsim 0.84$): This fact originates from the (i) smallness of the ratio \bar{J}/\bar{U} and (ii) absence of the d_{xy} -orbital hole-pocket, as explained in Ref. [24].

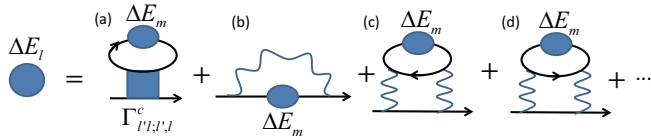


FIG. 5: Linearized self-consistent equation for $\Delta E_l(\mathbf{k})$ expanded up to the lowest order: (a) Hartree term, (b) MT-term, and (c)(d) AL-terms, respectively.

Here, we present an analytic explanation that the present self-consistent C_2 self-energy analysis is essentially equivalent to the SC-VC theory. Figure 5 shows the diagrammatic expression of the self-energy in Eq. (2), by expanding the right-hand-side with respect to $\Delta E_l = \Delta \Sigma_l$: (a), (b), and (c),(d) corresponds to the Hartree term, the Maki-Thompson (MT) term, and the AL-terms, respectively. We calculated these diagrams, and verified that the AL-terms give the dominant contribution. In the present theory, the higher-order MT- and AL-terms are included, whereas the feedback from the enhanced orbital susceptibility into the VC is absent.

From Fig. 5, the linearized self-consistent equation for ΔE_l ($l = 2, 3$) is obtained as

$$\lambda \Delta E_l(\mathbf{k}) \approx T \sum_{\mathbf{k}} \{U \{G_l(\mathbf{k})\}^2 \Delta E_l(\mathbf{k})$$

$$+ (2U' - J) \{G_{5-l}(\mathbf{k})\}^2 \Delta E_{5-l}(\mathbf{k})\} \quad (5)$$

$$+ T \sum_q (G_l(\mathbf{k} + \mathbf{q}) + G_l(\mathbf{k} - \mathbf{q})) \frac{3}{2} \{V_l^s(\mathbf{q})\}^2 \Lambda_l(\Delta E; \mathbf{q}),$$

where we assumed the orbital-diagonal \hat{G} and \hat{V}^s approximately, and $\Lambda_l(\Delta E; \mathbf{q}) = -T \sum_p \{G_l(p)\}^2 G_l(p + \mathbf{q}) \Delta E_l(\mathbf{p})$ is the three-point vertex. The MT-term is dropped in Eq. (5). The eigenvalue λ exceeds unity when the orbital order is realized. When we put $E_{xz}(\mathbf{k}) = -E_{yz}(\mathbf{k}) = \Delta E$ to simplify the discussion, and multiplying both sides of Eq. (5) by $-T \sum_{\mathbf{k}} \{G_l(\mathbf{k})\}^2$, we obtain

$$\lambda \chi^0(\mathbf{0}) \approx (2U' - J - U) \{\chi^0(\mathbf{0})\}^2 + X^c(\mathbf{0}), \quad (6)$$

where $\chi^0(\mathbf{0})$ is the bare-bubble and $X^c(\mathbf{0})$ is the charge-channel AL-VC for $l = 2$ or 3. Thus, the orbital order ($\lambda = 1$) is realized when $X^c(\mathbf{0}) > \chi^0(\mathbf{0}) - (U - 5J) \{\chi^0(\mathbf{0})\}^2 \sim 5J/U^2$ for $U = U' + 2J$, if we put $\chi^0(\mathbf{0}) \sim 1/U$ for a qualitative estimation. This result is consistent with the condition for $\alpha_C = 1$ in the SC-VC theory $X^c(\mathbf{0}) = (U - 5J)^{-1} - \chi^0(\mathbf{0}) \sim 5J/U^2$ for $J/U \ll 1$ [24]. Thus, the present theory is a natural extension of the SC-VC theory for the orbital-ordered state.

In the present study, we assumed that $z_l^{-1} = 1$ except for $l = 4$. If we put $z_l^{-1} = 1/z > 1$ for all l , the same numerical results are obtained by replacing r and T with r/z and Tz , respectively, as proved in Ref. [24]. Although the damping of the quasiparticle given by the imaginary part of the the self-energy is also neglected in the present study, this effect becomes small at sufficiently low temperatures, around the realistic $T_{\text{str}} \sim 100$ K.

Physically, the AL-terms in Fig. 5 (c) and (d) represent the enhancement of the C_2 -symmetric spin fluctuations due to the orbital order [39]. The essence of the present orbital-order mechanism is the strong positive feedback between the nematic orbital-order and C_2 -symmetric spin susceptibility, whereas it is missed in conventional mean-field approximations. The mechanism of the orbital fluctuations due to the AL-VC is confirmed by the renormalization group theory [40, 41]. The nematic p -orbital density wave (p -ODW) in cuprate superconductors is also explained by considering the AL-VC [42, 43].

In summary, we investigated the spontaneous symmetry breaking in the self-energy and susceptibility self-consistently, and explained the experimental characteristic in-plane anisotropies of the FSs and $\chi^s(\mathbf{q})$. In the FeSe model, the nematic orbital order is realized when the spin fluctuations are moderate ($\alpha_S \gtrsim 0.84$). The obtained FSs and $\Delta E_l(\mathbf{k})$ are qualitatively consistent with experiments. In LaFeAsO, in contrast, the orbital order is realized only when the spin fluctuations are strong. Since several key experimental results below T_{str} are well explained by the present study, it is considered that the orbital order/fluctuations originate from the Aslamazov-Larkin process [8, 9, 24].

We are grateful to Y. Matsuda and T. Shimojima for useful discussions. This study has been supported

by Grants-in-Aid for Scientific Research from MEXT of Japan.

-
- [1] R. M. Fernandes, L. H. VanBebber, S. Bhattacharya, P. Chandra, V. Keppens, D. Mandrus, M. A. McGuire, B. C. Sales, A. S. Sefat, and J. Schmalian, *Phys. Rev. Lett.* **105**, 157003 (2010).
- [2] F. Wang, S. Kivelson, and D.-H. Lee, arXiv:1501.00844.
- [3] A.V. Chubukov, R.M. Fernandes, and Joerg Schmalian, *Phys. Rev. B* **91**, 201105 (2015).
- [4] R. Yu, and Q. Si, *Phys. Rev. Lett.* **115**, 116401 (2015).
- [5] F. Krüger, S. Kumar, J. Zaanen, J. van den Brink, *Phys. Rev. B* **79**, 054504 (2009).
- [6] W. Lv, J. Wu, and P. Phillips, *Phys. Rev. B* **80**, 224506 (2009).
- [7] C.-C. Lee, W.-G. Yin, and W. Ku, *Phys. Rev. Lett.* **103**, 267001 (2009).
- [8] S. Onari and H. Kontani, *Phys. Rev. Lett.* **109**, 137001 (2012).
- [9] S. Onari, Y. Yamakawa, and H. Kontani, *Phys. Rev. Lett.* **112**, 187001 (2014).
- [10] S. Onari and H. Kontani, *Iron-Based Superconductivity*, (ed. P.D. Johnson, G. Xu, and W.-G. Yin, Springer-Verlag Berlin and Heidelberg GmbH & Co. K (2015)).
- [11] K. Jiang, J. Hu, H. Ding, and Z. Wang, arXiv:1508.00588.
- [12] M. Yoshizawa, D. Kimura, T. Chiba, S. Simayi, Y. Nakanishi, K. Kihou, C.-H. Lee, A. Iyo, H. Eisaki, M. Nakajima, and S. Uchida, *J. Phys. Soc. Jpn.* **81**, 024604 (2012).
- [13] A. E. Böhmer, P. Burger, F. Hardy, T. Wolf, P. Schweiss, R. Fromknecht, M. Reinecker, W. Schranz, and C. Meingast, *Phys. Rev. Lett.* **112**, 047001 (2014).
- [14] Y. Gallais, R. M. Fernandes, I. Paul, L. Chauviere, Y.-X. Yang, M.-A. Measson, M. Cazayous, A. Sacuto, D. Colson, and A. Forget, *Phys. Rev. Lett.* **111**, 267001 (2013).
- [15] H. Kontani and Y. Yamakawa, *Phys. Rev. Lett.* **113**, 047001 (2014).
- [16] M. Khodas, and A. Levchenko, *Phys. Rev. B* **91**, 235119 (2015).
- [17] J.-H. Chu, H.-H. Kuo, J. G. Analytis, and I. R. Fisher, *Science* **337**, 710 (2012).
- [18] A. E. Böhmer, T. Arai, F. Hardy, T. Hattori, T. Iye, T. Wolf, H. v. Lohneysen, K. Ishida, and C. Meingast, *Phys. Rev. Lett.* **114**, 027001 (2015).
- [19] S.-H. Baek, D. V. Efremov, J. M. Ok, J. S. Kim, Jeroen van den Brink, and B. Büchner, *Nature Mater.* **14**, 210 (2015).
- [20] M. C. Rahn, R. A. Ewings, S. J. Clarke, and A. T. Boothroyd, *Phys. Rev. B* **91**, 180501(R) (2015).
- [21] Q. Wang, Y. Shen, B. Pan, Y. Hao, M. Ma, F. Zhou, P. Steffens, K. Schmalzl, T. R. Forrest, M. Abdel-Hafiez, D. A. Chareev, A. N. Vasiliev, P. Bourges, Y. Sidis, H. Cao, and J. Zhao, arXiv:1502.07544.
- [22] Y. Nakai, S. Kitagawa, T. Iye, K. Ishida, Y. Kamihara, M. Hirano, and H. Hosono, *Phys. Rev. B* **85**, 134408 (2012).
- [23] F. L. Ning, K. Ahilan, T. Imai, A. S. Sefat, M. A. McGuire, B. C. Sales, D. Mandrus, P. Cheng, B. Shen, and H.-H. Wen, *Phys. Rev. Lett.* **104**, 037001 (2010).
- [24] Y. Yamakawa, S. Onari and H. Kontani, arXiv:1509.01161.
- [25] M. Yi, D. Lu, J.-H. Chu, J. G. Analytis, A. P. Sorini, A. F. Kemper, B. Moritz, S.-K. Mo, R. G. Moore, M. Hashimoto, W.-S. Lee, Z. Hussain, T. P. Devereaux, I. R. Fisher, and Z.-X. Shen, *Proc. Natl. Acad. Sci. USA* **108**, 6878 (2011).
- [26] Y. Zhang, C. He, Z. R. Ye, J. Jiang, F. Chen, M. Xu, Q. Ge, B. P. Xie, J. Wei, M. Aeschlimann, X. Y. Cui, M. Shi, J. P. Hu, and D. L. Feng, *Phys. Rev. B* **85**, 085121 (2012).
- [27] J. Maletz, V. B. Zabolotnyy, D. V. Evtushinsky, S. Thirupathaiiah, A. U. B. Wolter, L. Harnagea, A. N. Yaresko, A. N. Vasiliev, D. A. Chareev, A. E. Böhmer, F. Hardy, T. Wolf, C. Meingast, E. D. L. Rienks, B. Büchner, and S. V. Borisenko, *Phys. Rev. B* **89**, 220506(R) (2014).
- [28] K. Nakayama, Y. Miyata, G. N. Phan, T. Sato, Y. Tanabe, T. Urata, K. Tanigaki, and T. Takahashi, *Phys. Rev. Lett.* **113**, 237001 (2014).
- [29] M. D. Watson, T. K. Kim, A. A. Haghighirad, N. R. Davies, A. McCollam, A. Narayanan, S. F. Blake, Y. L. Chen, S. Ghannadzadeh, A. J. Schofield, M. Hoesch, C. Meingast, T. Wolf, and A. I. Coldea, *Phys. Rev. B* **91**, 155106 (2015).
- [30] T. Shimojima, Y. Suzuki, T. Sonobe, A. Nakamura, M. Sakano, J. Omachi, K. Yoshioka, M. Kuwata-Gonokami, K. Ono, H. Kumigashira, A. E. Böhmer, F. Hardy, T. Wolf, C. Meingast, H. v. Lohneysen, H. Ikeda, and K. Ishizaka, *Phys. Rev. B* **90**, 121111(R) (2014).
- [31] P. Zhang, T. Qian, P. Richard, X. P. Wang, H. Miao, B. Q. Lv, B. B. Fu, T. Wolf, C. Meingast, X. X. Wu, Z. Q. Wang, J. P. Hu, and H. Ding, *Phys. Rev. B* **91**, 214503 (2015).
- [32] Y. Zhang, M. Yi, Z.-K. Liu, W. Li, J. J. Lee, R. G. Moore, M. Hashimoto, N. Masamichi, H. Eisaki, S. -K. Mo, Z. Hussain, T. P. Devereaux, Z.-X. Shen, and D. H. Lu, arXiv:1503.01556.
- [33] Y. Suzuki, T. Shimojima, T. Sonobe, A. Nakamura, M. Sakano, H. Tsuji, J. Omachi, K. Yoshioka, M. Kuwata-Gonokami, T. Watashige, R. Kobayashi, S. Kasahara, T. Shibauchi, Y. Matsuda, Y. Yamakawa, H. Kontani, and K. Ishizaka, arXiv:1504.00980.
- [34] M. D. Watson, T. K. Kim, A. A. Haghighirad, S. F. Blake, N. R. Davies, M. Hoesch, T. Wolf, and A. I. Coldea, arXiv:1508.05016.
- [35] S.Y. Tan, Y. Fang, D.H. Xie, W. Feng, C.H. P. Wen, Q. Song, W. Zhang, Q.Y. Chen, Y. Zhang, L.Z. Luo, B.P. Xie, D.L. Feng, and X.C. Lai, arXiv:1508.07458.
- [36] S. Kasahara, T. Watashige, T. Hanaguri, Y. Kohsaka, T. Yamashita, Y. Shimoyama, Y. Mizukami, R. Endo, H. Ikeda, K. Aoyama, T. Terashima, S. Uji, T. Wolf, H. v. Lohneysen, T. Shibauchi, Y. Matsuda, *Proc. Natl. Acad. Sci. USA* **46**, 16309 (2014).
- [37] T. Miyake, K. Nakamura, R. Arita, and M. Imada, *J. Phys. Soc. Jpn.* **79**, 044705 (2010).
- [38] We verified that the critical value of r for the orbital order is slightly enlarged if Eq. (4) is replaced with $\Delta\Sigma_l(\mathbf{k}, \epsilon_n) = \{\Sigma_{l,l}(\mathbf{k}, \epsilon_n) - \Sigma_l^{A_{1g}}(\mathbf{k}, \epsilon_n)\}$.
- [39] H. Kontani, T. Saito, and S. Onari, *Phys. Rev. B* **84**, 024528 (2011).
- [40] M. Tsuchiizu, Y. Ohno, S. Onari, and H. Kontani, *Phys. Rev. Lett.* **111**, 057003 (2013).
- [41] M. Tsuchiizu, Y. Yamakawa, S. Onari, Y. Ohno, and H. Kontani, *Phys. Rev. B* **91**, 155103 (2015).

- [42] Y. Yamakawa and H. Kontani, Phys. Rev. Lett. **114**, 257001 (2015).
- [43] M. Tsuchiizu, Y. Yamakawa and H. Kontani, arXiv:1508.07218.